Neoplasia • Vol. 8, No. 1, January 2006, pp. 18–30 18

www.neoplasia.com

Anti-EphA2 Antibodies Decrease EphA2 Protein Levels in Murine CT26 Colorectal and Human MDA-231 Breast Tumors But Do Not Inhibit Tumor Growth

David Kiewlich[*,1], *Jianhuan Zhang*[*,1], *Cynthia Gross*[†], *Wei Xia*[†], *Brent Larsen*[†], *Ronald R. Cobb*[†], *Sandra Biroc*[†], *Jian-Ming Gu*[†], *Takashi Sato*[†], *David R. Light*[†], *Tara Heitner*[†], *Joerg Willuda*[‡], *David Vogel*[†], *Felipe Monteclaro*[†], *Andrzej Citkowicz*[†], *Steve R. Roffler*[§] *and Deborah A. Zajchowski**

*Corporate Research Oncology, Berlex Biosciences, Richmond, CA 94804, USA; [†]Research Center, Berlex Biosciences, Richmond, CA 94804, USA; [‡]Corporate Research Oncology, Schering AG, Müllerstraße 170-178, Berlin 13353, Germany; [§]Institute of Biomedical Sciences, Academia Sinica, Taipei, Taiwan

Abstract

The EphA2 receptor tyrosine kinase has been shown to be over-expressed in cancer and a monoclonal antibody (mAb) that activates and down-modulates EphA2 was reported to inhibit the growth of human breast and lung tumor xenografts in nude mice. Reduction of EphA2 levels by treatment with anti-EphA2 siRNA also inhibited tumor growth, suggesting that the anti-tumor effects of these agents are mediated by decreasing the levels of EphA2. As these studies employed human tumor xenograft models in nude mice with reagents whose cross-reactivity with murine EphA2 is unknown, we generated a mAb (Ab20) that preferentially binds, activates, and induces the degradation of murine EphA2. Treatment of established murine CT26 colorectal tumors with Ab20 reduced EphA2 protein levels to ~12% of control tumor levels, yet had no effect on tumor growth. CT26 tumor cell colonization of the lung was also not affected by Ab20 administration despite having barely detectable levels of EphA2. We also generated and tested a potent agonistic mAb against human EphA2 (1G9-H7). No inhibition of human MDA-231 breast tumor xenograft growth was observed despite evidence for >85% reduction of EphA2 protein levels in the tumors. These results suggest that molecular characteristics of the tumors in addition to EphA2 over-expression may be important for predicting responsiveness to EphA2-directed therapies.
Neoplasia (2006) **8,** 18–30

Keywords: EphA2, ephrinA1, antibodies, colorectal cancer, breast cancer.

Introduction

EphA2 is one of 16 related receptor tyrosine kinases that are activated by membrane-associated ligands known as ephrins (for review, see Refs. [1,2]). EphA2 protein levels have been reported to be elevated in breast cancer [3], prostate cancer [4], ovarian cancer [5], non–small cell lung cancer (NSCLC) [6], gastric cancer [7], squamous cervical carcinoma (SCC) [8], and esophageal squamous cell carcinoma (ESCC) [9], as well as in vertical growth-phase melanomas [10]. EphA2 is proposed to be a potential target for cancer therapy, as overexpression of EphA2 is significantly correlated with shorter overall survival in NSCLC [6], ESCC [9], SCC [8], and ovarian cancer [5], and with cancer progression and metastasis in colorectal cancer [11].

Although EphA2 protein levels are elevated in tumors, the EphA2 phosphorylation state in MDA-MB-231 breast cancer cells was found to be *lower* than that in "normal" MCF10A mammary epithelial cells, suggesting that reduced signaling through this pathway occurs in tumor cells that overexpress EphA2 [12]. Because cell–cell interaction is necessary to trigger ligand-dependent EphA2 phosphorylation, it was proposed that tumor cells either do not express appropriate ligands (i.e., ephrinA1–A5) or cannot form contacts that enable productive ephrinA–EphA2 interaction. Subsequent studies tested the hypothesis that exposure to ligand mimetics could inhibit tumor-associated phenotypes. Thus, dimerization of the ephrinA1 ligand by fusion to the Fc portion of human IgG_1 [i.e., ephrinA1-Fc (EA1-Fc)] was shown to trigger rapid EphA2 phosphorylation and receptor downmodulation in MDA-MB-231 breast [12,13] and PC-3 prostate [14] cancer cells. EA1-Fc treatment of PC-3 cells inhibited cell spreading on fibronectin, caused dephosphorylation/inactivation of focal adhesion kinase, and decreased clonal cell growth [14,15]. Monoclonal antibodies (mAbs) that induced EphA2 phosphorylation in MDA-MB-231 breast cancer cells—but not those lacking agonist activity—reduced cell piling in monolayer culture, inhibited anchorage-independent growth, and blocked invasive

Address all correspondence to: Deborah A. Zajchowski, Corporate Research Oncology, Berlex Biosciences, 2600 Hilltop Drive, Richmond, CA 94804.
E-mail: deb_zajchowski@berlex.com
[1]David Kiewlich and Jianhuan Zhang contributed equally to this work.
Received 18 August 2005; Revised 28 October 2005; Accepted 31 October 2005.

DOI 10.1593/neo.05544

outgrowth in Matrigel [13]. The agonistic mAb EA2 was also shown to inhibit the growth of MDA-MB-231 and A549 lung tumor xenografts in nude mice [16]. In such study, the tumor growth–inhibitory effects of antibody treatment were attributed to decreased EphA2 protein levels induced by receptor activation and degradation.

Reduction of EphA2 levels through treatment with anti-EphA2 antisense oligonucleotides (ASO) or siRNA has also been reported to inhibit *in vitro* tumor cell phenotypes. The invasive behavior of uveal melanoma cells, resembling vasculogenic mimicry [17] and MDA-MB-231 growth in soft agar [13], was inhibited by ASO-mediated knockdown of EphA2 expression. Pancreatic tumor cell invasion, migration, and *in vivo* tumor formation [18] were suppressed by siRNA that targeted EphA2. The observed effectiveness of both EphA2 agonists and ASO/siRNA suggested that antitumor effects were mediated by decreasing the levels of EphA2.

In addition to roles in tumor cell invasion, migration, adhesion, and survival, EphA2 has also been reported to be important in tumor angiogenesis [19] and in immune (i.e., dendritic) cell function [20,21]. Indeed, one of the EphA2 ligands, ephrinA1, was originally identified as an angiogenic factor produced by tumor necrosis factor α–stimulated endothelial cells [22]. It is unclear whether potential contribution to the growth of EphA2 activity from the murine host (i.e., endothelial, stromal, and immune cells) was impacted in the abovementioned studies. Those studies were performed with human tumor xenografts implanted in nude mice, and no data regarding cross-reactivity for murine EphA2 of the anti-EphA2 siRNA or agonistic antibodies were reported. We have therefore generated mAbs that preferentially target the murine EphA2 protein (Ab20) to determine the efficacy of anti-EphA2 therapy in a syngeneic tumor model, where both tumor and host cells are of murine origin. We have also generated an antibody that targets the human EphA2 receptor (1G9-H7). Both of these antibodies are potent EphA2 agonists and elicit the rapid phosphorylation and downmodulation of the receptor at concentrations similar to those of the dimeric ephrinA1 ligand. However, these antibodies did not impact the growth of either the murine syngeneic tumor or the human tumor xenograft despite causing substantial reduction in the levels of EphA2 protein.

Materials and Methods

Cell Lines and Culture Conditions

Human breast cancer (MDA-MB-134V1 and MCF7), murine colon cancer (CT-26), murine Lewis lung carcinoma (LLC1), and human HEK293 and HEK293-EBNA (293E) cell lines were obtained from the American Type Culture Collection (ATCC; Manassas, VA) and were cultured under conditions recommended by the supplier. Murine BWZ.36 thymoma (referred to as BWZ) cells are a derivative of $\alpha\beta$ BW5147 [23] and are kind gifts from Prof. Nilabh Shastri. MDA-MB-231 breast cancer cells (ATCC) were subcutaneously implanted in nude BALB/c mice, and one of the rapidly growing tumors was cultured *in vitro* to obtain MDA-231MT-1, which was used in the studies described in this publication (referred to as MDA-231). No significant differences were noted between the *in vivo*–selected cells and the parental population in *in vitro* characteristics, such as migration, invasion, or gene expression profiles as previously reported [24]. MDA-231 cells were cultured in alpha-modified minimal essential medium supplemented with 2.0 mM glutamine, 0.1 mM minimal essential amino acids, 1.0 mM sodium pyruvate (all from Invitrogen, Carlsbad, CA), 1.0 μg/ml insulin (Sigma, St. Louis, MO), and 10% fetal calf serum (FCS; SeraCare Life Sciences, Inc., Oceanside, CA).

HEK293 cells were transfected using Lipofectamine 2000 (Invitrogen) with pcDNA6-EphA2 [pcDNA6 (Invitrogen) encoding the full-length sequence–confirmed EphA2 protein] and were selected with BlasticidinS (Invitrogen). The 293-EphA2 cells used in this study were the progeny of a single cell clone, whose expression of EphA2 was verified by immunoblot, fluorescence-activated cell sorter (FACS), and immunocytochemical analyses.

Animals

Eight- to 10-week-old female nude mice (nu/nu) (Simonsen, Gilroy, CA) were used for the orthotopic MDA-231 human tumor xenograft model, and 6- to 8-week-old female BALB/c mice (Charles River, Hollister, CA) were used for the CT26 syngeneic tumor model. Mice were subcutaneously implanted with an electronic identification transponder (Biomedic Data Systems, Seaford, DE) and were housed in facilities approved by the American Association for Accreditation of Laboratory Animal Care. The Berlex Biosciences Animal Care and Use Committee approved all experimental designs. For use in animal experiments, all antibodies were confirmed to have endotoxin levels of less than 20 EU per daily dose (Nelson Laboratories, Inc., Salt Lake City, UT).

Recombinant Proteins and Antibody Reagents

Human EphA1-Fc, mEphA2-Fc, mEphA3-Fc, mEphA4-Fc, rEphA5-Fc, mEphA6-Fc, mEphA7-Fc, mEphA8-Fc, and mEA1-Fc were purchased from R&D Systems (Minneapolis, MN), and human IgG Fc fragment was purchased from Rockland Immunochemicals, Inc. (Gilbertsville, PA). Human EphA2-ECD was generated by transfecting 293E cells with pCEP4 encoding an N-terminal IgK signal sequence and a C-terminal V5/His6–tagged EphA2-ECD (amino acid sequences 23–524). Following growth in Gibco P6 media (Invitrogen), cells were pelleted and 9L cells of a supernatant containing EphA2 were processed. The protein was purified using Ni–NTA agarose (Qiagen, Hilden, Germany) and subsequent gel filtration using Superdex200. The protein was shown to have greater than 90% purity by analytic size exclusion chromatography and sodium dodecyl sulfate–polyacrylamide gel electrophoresis (SDS-PAGE).

Anti-EphA2 antibody C-20 and horseradish peroxidase (HRP)–conjugated anti-rabbit and anti-mouse IgG (Santa Cruz Biotechnology, Santa Cruz, CA) and anti–β-actin antibody clone AC-40 (Sigma-Aldrich, St. Louis, MO) were used in this study. The anti–human EphA2 antibody 355A93 (mAb A93, IgG_{2a}, and kappa) used in immunoprecipitation applications

was generated by the immunization of Swiss/Webster mice with pcDNA6-EphA2 and by further boosting with purified EphA2-ECD. Spleen and lymph nodes were harvested to create hybridomas (Strategic Biosolutions, Newark, DE). The antibody used to detect phosphotyrosine (4G10) was purchased from Upstate Biotechnology (Waltham, MA); Alexa488 or Alexa546 goat anti-human and anti-mouse IgG were from Molecular Probes (Eugene, OR). Isotype control IgG_{2b} and IgG_3 murine antibodies were purchased from Rockland Immunochemicals, Inc., and purified by anion exchange chromatography (Strong Basic Anion Exchanger Q15X; Sartorius AG, Goettingen, Germany).

Generation of Murine EphA2-Selective Antibodies

The human combinatorial antibody library HuCAL Gold Fab library (Morphosys, Martinsried, Germany), which was generated by transferring heavy- and light-chain variable regions from a previously constructed single-chain Fv library [25], was used for panning experiments with the mEphA2-Fc antigen. The HuCAL Gold Fab display library contains 2.1×10^{10} different human antibody fragments. The panning process was performed as previously described [26,27]. Briefly, wells of a 96-well plate were coated with 300 μl of recombinant mEphA2-Fc [50 μg/ml in phosphate-buffered saline (PBS); R&D Systems], and three rounds of panning were completed. After several washings, phages were eluted with dithiothreitol and amplified, and Fab-encoding fragments from the second and third rounds of panning were excised as a pool and cloned into the pMorph_x9_dHLX_MS format for screening. The dHLX format enables dimerization of Fabs and is based on a human-derived self-assembling polypeptide derived from the tetramerization domain of the human transcription factor p53 [28]. F′-negative TG1 was transformed with Fab-dHLX clones, and 744 single clones were screened in a 96-well plate format. Periplasmic extracts from positive unique clones based on DNA sequence analysis were then prepared as previously described [26] and analyzed by direct enzyme-linked immunosorbent assay (ELISA) on recombinant mEphA2-Fc by standard methods [27]. Positive Fab-HLX was purified and tested for binding to EphA2-expressing cells in FACS analyses. Confirmed positives were converted to IgG_3 format by subcloning into the pMorph_h/m_IgG3_1 and pMorph_h/m_IgGκ_ or pMorph_h/m_IgG λ_ expression vectors and were subsequently expressed in CHO cells. These expression vectors yielded mouse chimeric antibodies with murine constant regions and human variable regions.

Generation of Human EphA2 Antibodies

Human lung carcinoma cell lines with different invasive and metastatic capabilities (CL1-0 and its sublines CL1-1 to CL1-5) have been described [29]. mAbs against human lung cancer cells were produced by immunizing BALB/c mice with highly metastatic CL1-5 cells and by selecting antibodies that preferentially bound CL1-5 cells compared with CL1-0 cells [30]. mAb 1G9-H7 was found to bind EphA2 by the immunoprecipitation of solubilized CL1-5 cell membrane proteins followed by in-gel digestion and mass spectrometric analysis, as described [31].

FACS Binding Analyses

Cells were cultured to approximately 80% confluency, detached with Versene or Cell Dissociation Buffer (Invitrogen), centrifuged, and resuspended in ice-cold PBS. Cells [1×10^5 cells/well in 96-well round-bottom Pro-Bind Assay plates Recton Dickinson Labware (Falcon, Franklin Lakes, NJ) analyzed using PCA-96 FACS instrument (Guava, Hayward, CA), or 1×10^6/cells/1.5-ml microtube analyzed using FACSCalibur (BD Biosciences, Franklin Lakes, NJ)] were centrifuged and incubated with 200 μl of primary antibody (diluted in PBS at concentrations indicated in figure legends) for 1 hour at 4°C, with constant agitation. Following three washes with ice-cold PBS, cells were resuspended in 200 μl of either anti-mouse or anti-human IgG Alexa546 (1:500 in PBS for PCA-96 analysis) or anti-mouse or anti-human IgG Alexa488 (1:500 in PBS for FACSCalibur analysis) and incubated for 30 minutes at 4°C, with constant agitation. Following three washes with ice-cold PBS, cells were resuspended in 200 μl of PBS containing 2 μg/ml 7AAD (Molecular Probes) for PCA-96 analysis, or in 2 μg/ml propidium iodide (Molecular Probes) for FACSCalibur analysis. Samples were analyzed by the 96-well PCA-96 FACS instrument using the preset "Guava Express" software, or by the FACSCalibur machine using the preset "Cell Quest" software.

EphA2 Activation Studies

MDA-231 cells (6×10^4 cells/well) or CT26 cells (2×10^5 cells/well) were seeded in a six-well plate. Two days later, the medium was removed and replaced with FBS-free medium (for CT26) or fresh medium (for MDA-231), including EA1-Fc or antibodies, at the concentrations indicated in the figure legends. Cells were incubated at 37°C for the indicated times, rinsed once with cold PBS, and lysed in RIPA-PP [modified RIPA buffer (0.5% deoxycholate, 0.1% SDS, 1% Triton X-100, and 5 mM EDTA in PBS, pH 8.0), supplemented with protease inhibitors (Complete Tablet EDTA-free; Roche Diagnostics GmbH, Mannheim, Germany) and 5 mM sodium vanadate (Aldrich Chem. Co., Milwaukee, WI)]. Samples were sonicated, protein concentration was determined by BCA (Pierce, Rockford IL), and EphA2 was immunoprecipitated overnight at 4°C in a final volume of 600 μl. For MDA-231, 500 μg of total protein was incubated with 5 μg of A93 anti-EphA2 antibody; for CT26, 450 μg of protein with 6 μg of anti-EphA2 (C-20) antibody and 30 μl of protein A (for C-20) or protein G (for A93) beads (20 mg/ml; Amersham Biosciences Corp., Piscataway, NJ) was diluted in RIPA-PP buffer. Beads were washed three times with HNTG (25 mM HEPES, pH 7.4, 150 mM NaCl, 1% Triton X-100, and 5% glycerol) buffer, eluted with hot SDS-PAGE sample buffer, and subjected to immunolot analysis.

Western Blot Analysis

Approximately 80% confluent 293, 293EphA2, BWZ, CT26, and LLC1 cells were lysed in RIPA-PP buffer, sonicated, and denatured by boiling in SDS-PAGE sample buffer (Invitrogen) with 10% Bond-Breaker TCEP Solution (Pierce), and the components were resolved by electrophoresis in 4% to 12% or in 4% to 20% Tris–glycine gels (Cambrex

BioScience Rockland, Inc., Rockland, ME). Proteins were transferred to a 0.2-μm nitrocellulose membrane (Invitrogen) and blocked with 5% milk powder in StartingBlock (PBS formulation; Pierce) with 0.1% Tween-20 (Sigma) for 1 hour at room temperature (RT), with constant agitation. Primary antibodies [anti-EphA2 (C-20; 0.05 μg/ml), anti-phosphotyrosine (4G10; 0.01 μg/ml), and anti–β-actin (0.05 μg/ml)] were diluted in blocking buffer and incubated for 1 hour at RT, with constant agitation. After washing with PBST (PBS with 0.1% Tween-20), the blots were incubated with either anti–rabbit IgG–HRP (1:5000) or anti–mouse IgG–HRP (1:5000) in blocking buffer for 1 hour at RT. Blots were washed with PBST, rinsed once with distilled water, and processed for the detection of HRP by incubating with Super-Signal West Pico (Pierce). Where indicated, EphA2 levels were determined by scanning densitometry using the Gel Doc system (Bio-Rad, Hercules, CA). To verify equivalent sample loading, the blots were stripped and reprobed for β-actin.

CT26 Invasion Assay

CT26 cells were cultured to approximately 80% confluency, detached with Cell Dissociate Buffer, centrifuged, and resuspended in growth medium without FBS. Cells were incubated at RT with mIgG, Ab20, Fc, or EA1-Fc (1 or 5 μg/ml) for 30 minutes before layering 2×10^5 cells/500 μl in triplicate onto a rehydrated Matrigel-coated filter on the top chamber of a Biocoat Tumor Invasion System 24-Multiwell Insert Plate (Becton Dickinson, Bedford, MA). A total of 750 μl of basal medium containing 5% FCS was added to the bottom chamber, and the plate was incubated at 37°C in a 5% CO_2 incubator for 19 hours. Cells at the bottom of the filter were fixed with Diff-Quick (Dade Behring, Inc., Dudingen, Switzerland) for 2 minutes and stained with Syto 13 (Molecular Probes) for 30 minutes at 37°C. The fluorescence intensity of invaded cells was measured with a Victor Fluorometer (Perkin-Elmer, Boston, MA) and corrected by subtracting the fluorescence measurement from chambers where no cells were added.

In Vivo *Efficacy Studies*

MDA-231 tumor xenografts MDA-231 cells [2×10^6 cells/mouse mixed 1:1 with Matrigel (BD Biosciences, Bedford, MA) in a volume of 40 μl] were injected into the left inguinal mammary fat pad of female athymic mice under light isoflurane anesthesia. The progress of tumor growth was measured with calipers in two perpendicular directions and calculated using the formula $V = WWL(0.5)$, where V = volume, W = the shortest diameter, and L = the longest diameter. Three weeks after cell inoculation (tumors, 65–150 mm^3), mice were sorted into groups of 12 and treatment was initiated. Mice were injected intraperitoneally every second or third day with 125 μg (in 125 μl) of either 1G9-H7, isotype control antibody IgG_{2b}, or PBS. One day after the last antibody dose, mice were euthanized, and tumors were excised, weighed, and snap-frozen in liquid nitrogen.

CT26 syngeneic tumors CT26 cells (1×10^6 cells/mouse in 100 μl of PBS) were implanted subcutaneously into the dorsal flank of female BALB/c mice whose fur was shaved and depilated with Veet (Reckitt Benckiser, Inc., Wayne NJ). Tumor volume was estimated by caliper measurements twice a week. One week after cell inoculation (tumors, 50–100 mm^3) and every second or third day thereafter, mice (n = 20/group) were treated intraperitoneally with 125 μg (in 125 μl) of either Ab20 or control IgG_3 or antibody diluent (330 μM sodium acetate and 150 μM NaCl, pH 5.5) for a total of seven doses. One day after the final dose, mice were euthanized, and tumors were excised, weighed, and snap-frozen in liquid nitrogen.

CT26 lung colonization CT26 cells (5×10^5 cells/mouse in 100 μl of calcium/magnesium-free PBS containing 10 mM glucose) were injected in the lateral tail vein of BALB/c mice. Three hours before intravenous cell inoculation and every second or third day thereafter, mice (n = 20/group) were treated intraperitoneally with 125 μg (in 125 μl) of either Ab20 or control IgG_3. One set of age-matched mice was used for the determination of normal lung weight. Two days after the final antibody dose, all mice were euthanized by CO_2 asphyxiation, and the lungs were carefully dissected, weighed, and snap-frozen in liquid nitrogen or fixed in 4% paraformaldehyde in 3% sucrose buffer. Tumor burden was estimated by subtracting the normal lung weights of mice that received no CT26 cells from the lung weights of animals injected with CT26 tumor cells.

Tumor Tissue Extraction

Frozen tumors were fragmented with the aid of a Bessman tissue pulverizor (Spectrum Laboratories, Inc., Rancho Dominguez, CA) and transferred to precooled cryovials in a dry ice–ethanol bath. Approximately 100 to 300 mg of tumor was extracted in 1 ml of RIPA-PP buffer by adding two 1/4-in. ceramic beads and garnet sand (BIO 101, Inc., Carlsbad, CA) and by shaking the vials in the Fast Prep reciprocal shaker (Q-biogen, Irvine, CA) for 30 seconds at full speed in a cold room. The samples were centrifuged for 2 minutes at 15,000*g*, and the process was repeated. The supernatant was briefly sonicated, centrifuged for 5 minutes to clarify the lysate, quickly frozen, and stored at −80°C. For preparation of extracts from tumor-bearing lungs, the tissue was weighed and 10-fold excess RIPA-PP buffer was added before homogenizing with an Omni mixer (Omni International, London, UK). A total of 100 μl of this crude homogenate was further extracted and processed using the Fast Prep protocol described above.

Statistical Analysis

Statistical analyses for *in vivo* tumor growth studies were performed with JMP 5.0 (SAS Institute, Inc., Cary, NC) using the Kruskal-Wallis test and the Wilcoxon nonparametric (Mann-Whitney U) analysis. Results from *in vitro* invasion studies were analyzed by an ANOVA unpaired test. $P < .05$ was considered significant.

Results

Generation of Antibodies against Murine EphA2

The HuCAL Gold Fab phage display library was screened for Fab antibody fragments that bound to the murine EphA2-

ECD fused to the human IgG_1 Fc (i.e., mEphA2-Fc). A total of 134 mEphA2-binding Fab clones was identified, and a diversity of 21 was determined after the comparison of heavy-chain sequences. Following additional screening analyses, Fab antibody fragments were converted to the IgG_3 format by subcloning, expressed in CHO cells, and the antibodies were purified.

The antibodies identified by binding to mEphA2-Fc were tested by FACS-based analyses for their ability to recognize native EphA2, which is highly expressed by murine CT26 colorectal and LLC1 cells (Figure 1*A*). The binding of one of these antibodies (Ab20) to CT26 cells—but not to BWZ cells, which do not express EphA2—is shown in Figure 1*B*. Although several antibodies bound to cell surface EphA2 as measured by mean fluorescence intensity, only Ab20 bound with an affinity similar to that of EA1-Fc (Figure 1*C*). The EC_{50} for Ab20 binding was 1.2 to 1.7 nM compared to 0.8 to 2.1 nM for EA1-Fc. Maximal binding was observed at antibody concentrations of 1 to 2 μg/ml (6–13 nM) compared with 0.5 to 1 μg/ml (4.5–9 nM) for EA1-Fc. Ab20 did not significantly interact with human EphA2 (hEphA2) on MDA-231 breast cancer cells (Figure 1*D*) or on 293 cells transfected with hEphA2 (data not shown), even though these human cell lines express similar or greater levels of EphA2 than those detected in CT26 and LLC1 (Figure 1*A*). These data suggest that Ab20 specifically recognizes murine—but not human—EphA2. This conclusion is supported by results from competitive binding studies, where mEphA2-Fc—but not hEphA2-ECD—competed for the binding of Ab20 to CT26 tumor cells (Figure 1*E*). None of the other EphA receptor–Fc fusions (murine EphA2, EphA3, EphA4, EphA6, EphA7, EphA8; rat EphA5; or human EphA1) interfered with

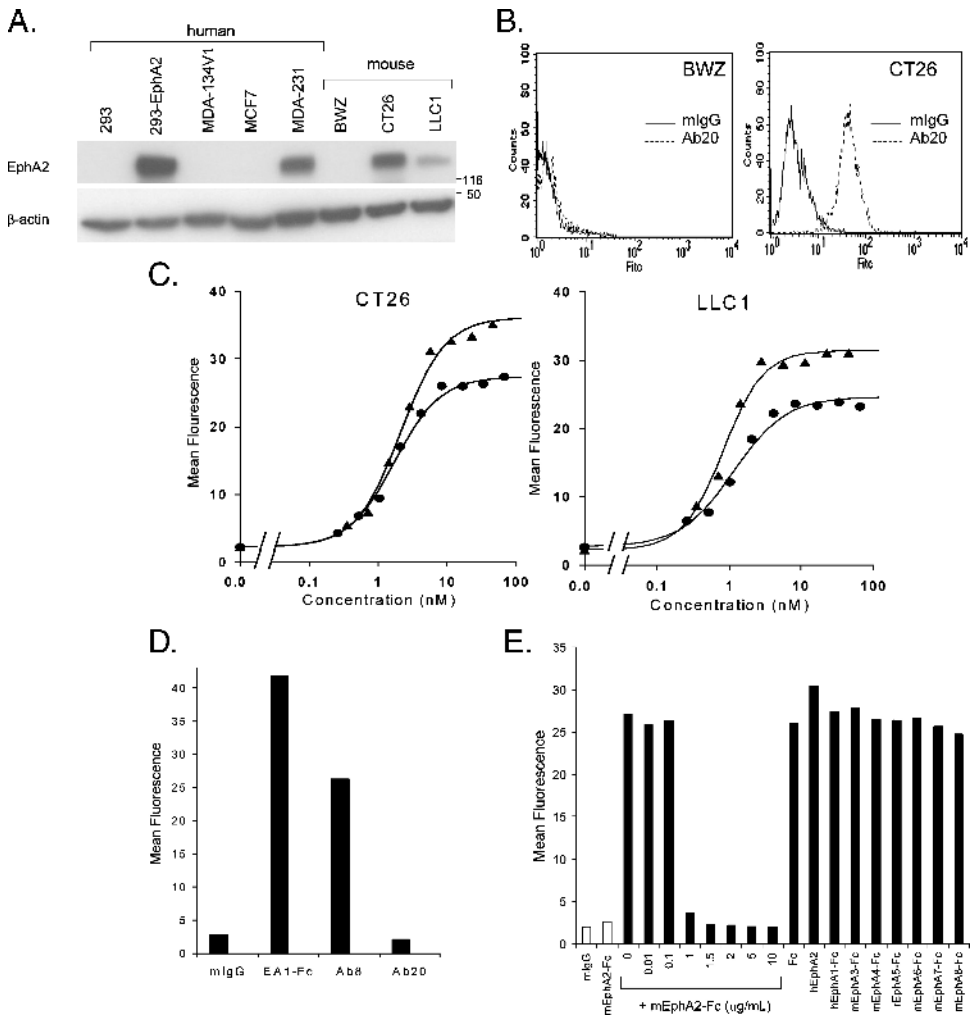

Figure 1. *EphA2 expression and FACS binding of Ab20 to cell surface EphA2 in murine and human cells. (A) Western blot analysis of total cell extracts (30 μg protein/lane) from indicated cell lines. EphA2 was detected with the C-20 antibody. Molecular weight standards (kDa) are indicated on the side. (B) CT26 or BWZ cells were incubated with 5 μg/ml mIgG (solid line) or Ab20 (dashed line) for 1 hour at 4°C, labeled with anti-mouse IgG Alexa488, and analyzed by FACS. Histograms of fluorescence intensity (FITC) versus cell number (counts) are shown. (C) CT26 or LLC1 cells were incubated with indicated concentrations of EA1-Fc (triangles) or Ab20 (circles) and treated as described in (B). The mean fluorescence for binding at each concentration is graphically shown. The average EC_{50} for Ab20 binding (n = 3) to CT26 is 1.94 ± 0.24 nM and to LLC1 is 1.52 ± 0.32 nM. EA1-Fc EC_{50} to CT26 is 2.1 nM and to LLC1 is 0.83 nM. (D) Human MDA-231 cell binding of indicated antibodies (5 μg/ml) or EA1-Fc (0.5 μg/ml) was measured as described in (B). (E) CT26 cells were incubated with Ab20 (1 μg/ml) in the presence of indicated concentrations of mEphA2-Fc or other EphA-Fc (10 μg/ml; solid bars). The binding of mIgG (1 μg/ml) or mEphA2-Fc (10 μg/ml) is represented by open bars. Representative data from at least two independent experiments are shown.*

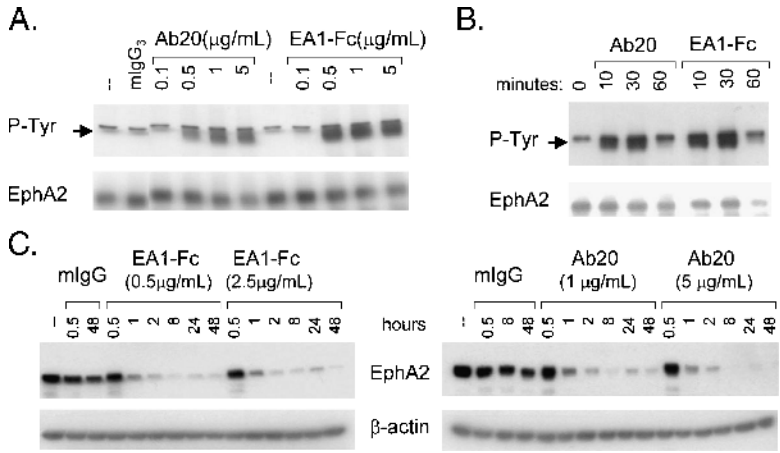

Figure 2. *Effect of Ab20 on the phosphorylation and degradation of EphA2 in CT26 cells. (A) CT26 cells were incubated with Ab20 or EA1-Fc at 37° C with indicated concentrations for 30 minutes or (B) with 1 μg/ml Ab20 or 0.5 μg/ml EA1-Fc for indicated times. Cell extracts were prepared in RIPA-PP buffer, and 450 μg of protein was immunoprecipitated with anti-EphA2 polyclonal antibody (C-20). Western blots were probed with anti-phosphotyrosine (4G10) and anti-EphA2 (C-20), respectively. Arrows indicate tyrosine-phosphorylated EphA2. (C) CT26 cells were treated with indicated concentrations of EA1-Fc or Ab20 for indicated times, and cell extracts (20 μg/lane) were evaluated by Western blot analysis for EphA2 and β-actin levels. Data shown are representative of at least two independent experiments.*

the binding of Ab20 to CT26 cells, suggesting that Ab20 is selective for murine EphA2.

Ab20 Is a Potent Agonist of Murine EphA2

The EphA2 agonistic potential of Ab20 was assayed by measuring EphA2 autophosphorylation in CT26 cells following 30 minutes of incubation with the antibody. EphA2 phosphorylation in response to Ab20 increased in a dose-dependent manner to levels comparable to those observed with maximally effective concentrations of EA1-Fc (Figure 2*A*). The EC_{50} values for EA1-Fc and Ab20 were also very similar at ~0.25 to 0.5 μg/ml (2–5 nM). The kinetics of phosphorylation elicited by Ab20 was also quite similar to that for EA1-Fc (Figure 2*B*), with maximal EphA2 phosphorylation observed within 15 minutes of incubation in both CT26 and LLC1 cells (data not shown). EA1-Fc and Ab20 also induced receptor degradation with similar kinetics (Figure 2*C*), rapidly reducing EphA2 protein levels within the first 2 hours of treatment and achieving ~80% reduction by 8 hours. Decreased levels of EphA2 were maintained for at least 48 hours.

Ab20 Inhibits CT26 Tumor Cell Invasion

The ability of Ab20 to interfere with CT26 tumor cell invasion through a reconstituted basement membrane (i.e., Matrigel) was evaluated using a modified Boyden chamber assay. Ab20 significantly reduced invasion by approximately two-fold at a concentration of 5 μg/ml (33 nM), whereas weaker inhibition, although not statistically significant, was observed with EA1-Fc treatment (Figure 3). No effect was observed with $mIgG_3$ or Fc controls. Ab20 caused no antiproliferative effects on CT26 growth in monolayer culture (data not shown).

Ab20 Treatment Reduces EphA2 Protein Levels in CT26 Tumor Xenografts But Does Not Affect Primary Tumor Growth or Lung Colony Formation

Given the strong agonistic activity of Ab20 in eliciting EphA2 phosphorylation and degradation in CT26 tumor cells, the effectiveness of Ab20 in controlling CT26 tumorigenicity in BALB/c mice was evaluated. Antibody administration was initiated 1 week after tumor cell implantation, when tumors were ~50 to 100 mm^3, and continued on a thrice-weekly injection schedule until mice were sacrificed ~24 hours after the final injection on day 22. No change in tumor growth kinetics was observed over the course of this treatment (Figure 4*A*). The histopathology and weight of the tumors from treated and untreated mice were not different (data not shown). It is also noteworthy that there were no

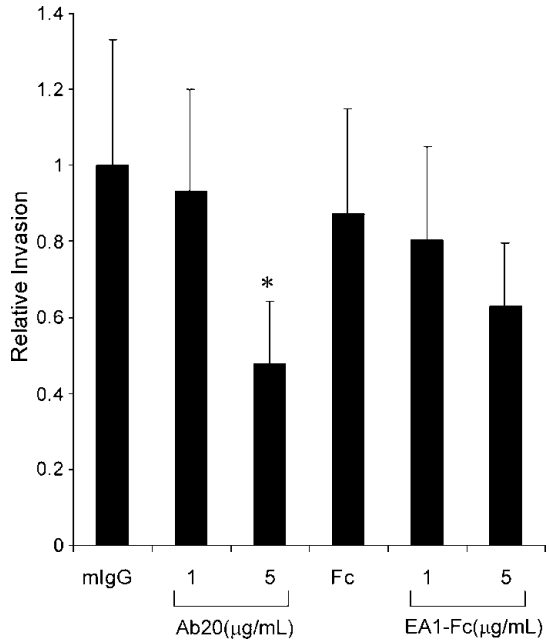

Figure 3. *Effect of Ab20 on CT26 tumor cell invasion. CT26 cells (2×10^5) were preincubated with Ab20 or EA1-Fc at RT for 30 minutes and plated onto Matrigel-coated membranes in a modified Boyden chamber. Cell invasion was measured after 19 hours of treatment. Data are the normalized and averaged results from four independent experiments. *Statistically significant at P < .05.*

apparent adverse effects of administering Ab20, as recorded by body weight measurements (data not shown).

To rule out the possibility that the concentrations of the Ab20 reaching the tumor were insufficient to induce phosphorylation and degradation, EphA2 levels were measured in all of the tumors. In every tumor excised from mice that received Ab20 treatment—but not in those from control mIgG$_3$– or vehicle-treated mice—EphA2 levels were markedly reduced (Figure 4*B*). The mean reduction was ~85%, clearly demonstrating that the Ab20 antibody was effective in reaching tumor mass and inducing the degradation of the EphA2 protein.

However, it was theoretically possible that Ab20 was ineffective in the early days of treatment and therefore could not affect these rapidly growing tumors. Such a delayed effectiveness might not be observed in tumors analyzed after 2 weeks of chronic antibody treatment. In a separate study, CT26 tumor–bearing mice were given a single injection of Ab20 and tumors were harvested 24 hours later. In this case, in EphA2 protein levels were reduced 80% to 85% (Figure 4*C*) and were therefore comparable to those observed following chronic dosing with the antibody, demonstrating the effectiveness of Ab20 in eliciting EphA2 degradation soon after treatment.

Because the *in vitro* efficacy data supported a role for EphA2 in the invasion of CT26 tumor cells, the ability of Ab20 to impact metastatic behavior, as measured by CT26 cell seeding and growth in the lung following tail vein injection, was also assessed. Fifteen days after injection, the CT26 tumor nodules accounted for nearly 50% of the total weight of the lung in the mIgG$_3$- and Ab20-treated mice (Figure 5*A*, *left side*). Histopathological examination confirmed that a large percentage of the lung parenchyma was effaced by multifocal to coalescing nodular neoplasms (data not shown). No significant effect on tumor burden was observed in mice treated with Ab20 (Figure 5*A*, *right side*), even though the antibodies were administered 3 hours prior to tumor cell inoculation. In addition, no effects of Ab20 administration on animal body weight were observed (data not shown).

The pharmacodynamic activity of Ab20 was verified by measuring EphA2 levels in the CT26 tumor nodules. Extracts prepared from lungs of treated and untreated mice were compared with those from mice that were not injected with CT26 tumor cells. In agreement with the reported expression of EphA2 mRNA in normal rat lung tissues [32], a low level of EphA2 protein was detectable in lungs from naïve mice (Figure 5*B*). The EphA2 levels detected in the lungs from mice injected with CT26 tumor cells were very high, as expected, due to the high expression of EphA2 in CT26 tumors. Importantly, tumors from Ab20-treated mice contained nearly undetectable levels of EphA2, consistent with an Ab20-mediated degradation of the protein.

Characterization of mAbs against hEphA2

Antibodies that recognize hEphA2 were generated through a cellular immunization strategy in a search for antigens that were overexpressed in highly metastatic human lung tumor cells (CL1-5) [30]. hEphA2 was identified as the antigen for the 1G9-H7 antibody following its immunoprecipitation from CL1-5 cells and liquid chromatography–mass spectrometry sequencing analysis. The specificity of 1G9-H7 for EphA2 was confirmed by its ability to only bind EphA2-expressing cells in FACS analyses (Figure 6*A*). The mean fluorescence intensity of 1G9-H7 binding to MDA-231, which expresses very high levels of EphA2 (Figure 1*A*),

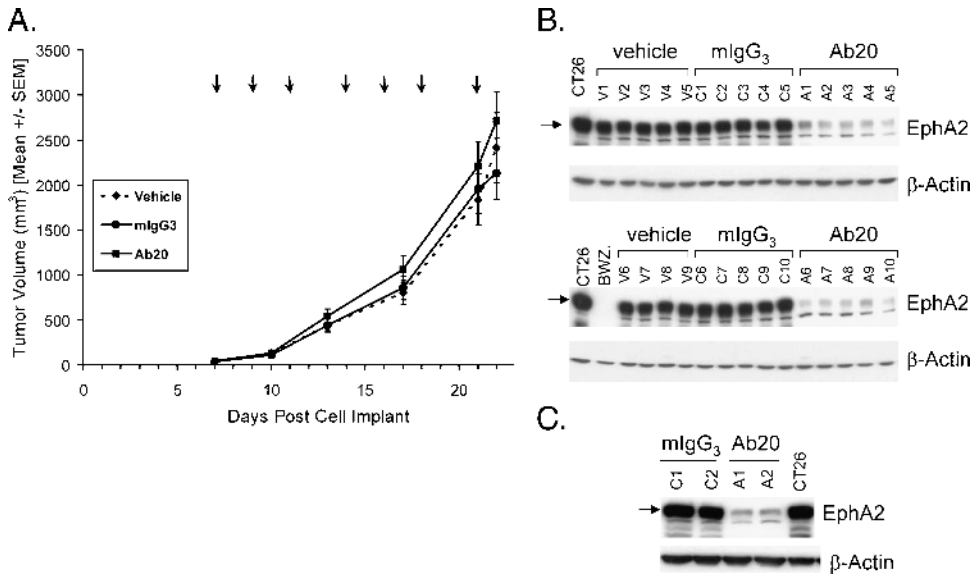

Figure 4. *Effect of Ab20 administration on subcutaneous CT26 tumor growth and EphA2 levels. (A) Mice bearing subcutaneous CT26 tumors (50–100 mm^3; n = 20/group) were treated with vehicle, mIgG$_3$, or Ab20 (125 μg/dose) according to the schedule shown (arrows). Mean tumor volumes are graphically represented. The corresponding tumor weights (g) were as follows: vehicle, 1.49 ± 0.22; mIgG$_3$, 1.35 ± 0.19; and Ab20, 1.77 ± 0.21. Error bars, SEM. (B) Western blot analysis of extracts (25 μg of protein) from subcutaneous CT26 tumors excised 1 day after the final treatment. EphA2 was detected with anti-EphA2 antibody C-20, and the data for half of the tumors from each group (vehicle, V1–V9; mIgG$_3$, C1–C10; and Ab20, A1–A10) are shown. Similar results were obtained with the remaining tumors. Average (± SD) EphA2 levels determined by densitometric scanning of the blots were as follows: vehicle, 9710 ± 1272; mIgG$_3$, 9674 ± 204; and Ab20, 1413 ± 979 arbitrary units. (C) CT26 tumor lysates from mice treated for 24 hours with mIgG$_3$ (C1 and C2) or Ab20 (A1 and A2) were analyzed as in (B).*

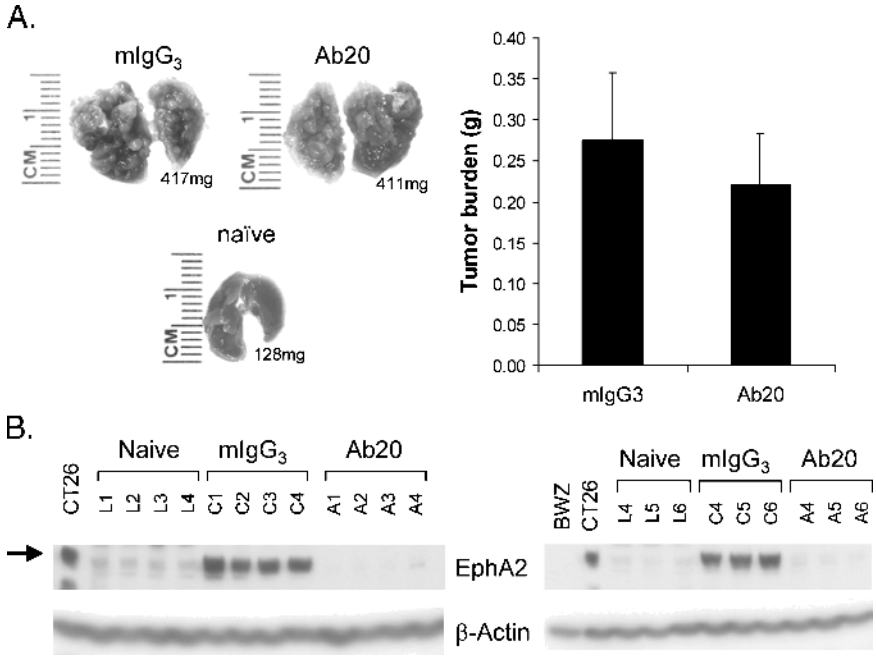

Figure 5. *Effect of Ab20 treatment on CT26 lung colonization and EphA2 levels. CT26 cells (5×10^5) were injected into the lateral tail vein of BALB/c mice. Three hours before intravenous cell inoculation and every second or third day thereafter, mice (n = 20/group) were treated intraperitoneally with 125 μg of either Ab20 or isotype-matched control mIgG3. (A) Left side: Photographic images are shown for a representative lung (corresponding weight also indicated) from each treatment group at the end of the study. (A) Right side: Average tumor burden [lung weight of CT26-injected mice minus the average weight of lungs from naïve mice (0.129 ± 0.013 g)] is graphically depicted. Error bars, SEM. (B) EphA2 levels in lung tissue extracts (50 μg protein/lane) from naïve (L1–L6)–, mIgG3 (C1–C6)–, and Ab20 (A1–A6)–treated CT26-bearing mice were analyzed by immunoblotting for EphA2 and β-actin levels.*

was much greater than that for MCF7 (with very low levels detected on long exposure of the blot; data not shown) and MDA-MB-134VI (with undetectable levels). A dose-dependent binding of 1G9-H7 to 293 cells stably transfected with hEphA2 (293-EphA2)—but no binding to the parental 293 cells—was observed (Figure 6*B*). The EC_{50} for 1G9-H7 binding to 293-EphA2 cells was 1.8 nM, and similar data were obtained for binding to EphA2 on MDA-231 cells (data not shown). EA1-Fc binds to MDA-231 and 293-EphA2 cells with similar potency (data not shown).

The potential species specificity of 1G9-H7 was addressed by measuring binding to mEphA2 on CT26 and LLC1 tumor cells. 1G9-H7 bound very well to hEphA2 on MDA-231 and 293-EphA2 cells, but weakly (or not at all) bound to mEphA2 on CT26 or LLC1 tumor cells (Figure 6*C*). In competitive binding studies, incubation with excess hEphA2-ECD—but not mEphA2-Fc—reduced 1G9-H7 binding to MDA-231 cells (Figure 6*D*). No competition for binding was observed with hEphA1 (Figure 6*D*), which was one of the most closely related EphA to EphA2 (i.e., 55.9% amino acid similarity in the extracelluar domain) or with any of the rodent EphAs (data not shown). These data indicate that 1G9-H7 preferentially binds human EphA2.

Antibody IG9-H7 Is a Potent Activator of hEphA2

The agonistic activity of 1G9-H7 was measured on MDA-231 cells in comparison to EA1-Fc following a 10-minute incubation. The level of EphA2 phosphorylation induced by 1G9-H7 treatment was ~40% to 50% of that observed with EA1-Fc (Figure 7, *A* and *B*), but was of similar potency (EC_{50} ~0.25 μg/ml or 1.7 nM; Figure 7*A*). The kinetics of EphA2 phosphorylation by EA1-Fc and 1G9-H7 was also very similar, with peak activation at approximately 10 minutes for both agonists (Figure 7*B*). Incubation with EA1-Fc or 1G9-H7 for longer times resulted in receptor degradation to levels that were barely detectable 8 hours after stimulation (Figure 7*C*), with very similar kinetics for the antibody and the dimeric ligand.

1G9-H7 Fails to Inhibit MDA-231 Tumor Growth But Dramatically Reduces Tumor EphA2 Levels

The antitumor effectiveness of the 1G9-H7 anti-EphA2 agonistic antibody was evaluated in MDA-231 tumor xenografts orthotopically implanted in the mammary fat pads of nu/nu mice. Antibody treatment was initiated when the tumors were 65 to 150 mm^3, and intraperitoneal injections were repeated thrice weekly over the course of the study until 24 hours before sacrifice. There was no effect of 1G9-H7 administration on the growth rate of MDA-231 tumors (Figure 8*A*). The histopathology and weight of the tumors from treated and untreated mice were also not different (data not shown).

The levels of EphA2 protein were measured in extracts from the excised tumors. There was little variation in the EphA2 levels in the tumors from the PBS and the isotype-matched IgG_{2b}-treated mice, but all of the tumors from 1G9-H7–treated mice had significantly lower (83%) levels of EphA2 than the controls (Figure 8*B*). These pharmacodynamic data show that the 1G9-H7 antibody displayed expected activity in the tumor but was unable to influence its growth.

Discussion

In this study, we describe the generation and characterization of two mAbs that are potent agonists of either the mouse or the human EphA2 receptor tyrosine kinase. Comparative analyses revealed that the Ab20 (mouse) and 1G9-H7 (human) antibodies are similar to the dimeric EA1-Fc ligand in their potency and kinetics of stimulating EphA2 phosphorylation and degradation. However, in spite of their efficiency in substantially reducing EphA2 levels in murine CT26 colorectal tumors and in human MDA-231 breast tumor xenografts, neither of these antibodies inhibited *in vivo* tumor growth.

Reported studies with agents that target EphA2 for degradation (i.e., agonistic antibodies and siRNA) were performed in human tumors that were xenografted onto immunocompromised mice. Therefore, the aim of our study was to evaluate the activity of an agonistic EphA2-targeting antibody in a murine syngeneic tumor model where effects on EphA2 function in both tumor and host cells (i.e., endothelial, stromal, and immune cells) would be potentially targeted. We selected the murine CT26 colorectal tumor model for these studies because these cells express very high levels of EphA2 protein and form rapidly growing, highly vascularized tumors in mice. Importantly, a recent study correlated the overexpression of the EphA2 protein in human colorectal carcinomas with cancer progression and metastasis [11], thereby providing a clinical rationale for testing therapeutic antibodies in this indication.

To evaluate the efficacy of an EphA2-targeting antibody in a murine syngeneic tumor model, we generated an antibody (Ab20) that specifically recognizes mEphA2 using phage display technology. The preferential affinity of Ab20 for mEphA2 was demonstrated by binding to EphA2-expressing—but not EphA2-negative—murine cell lines as well as competitive binding analyses. Only mEphA2-Fc was a competitive inhibitor of Ab20 binding to mEphA2 on cells. hEphA2 ECD, which shares 90% sequence similarity with the mEphA2 ECD and a panel of six other rodent EphA ECD–Fc fusion proteins, which are 50% to 55% homologous to the EphA2 ECD, were all inactive in this competitive binding assay.

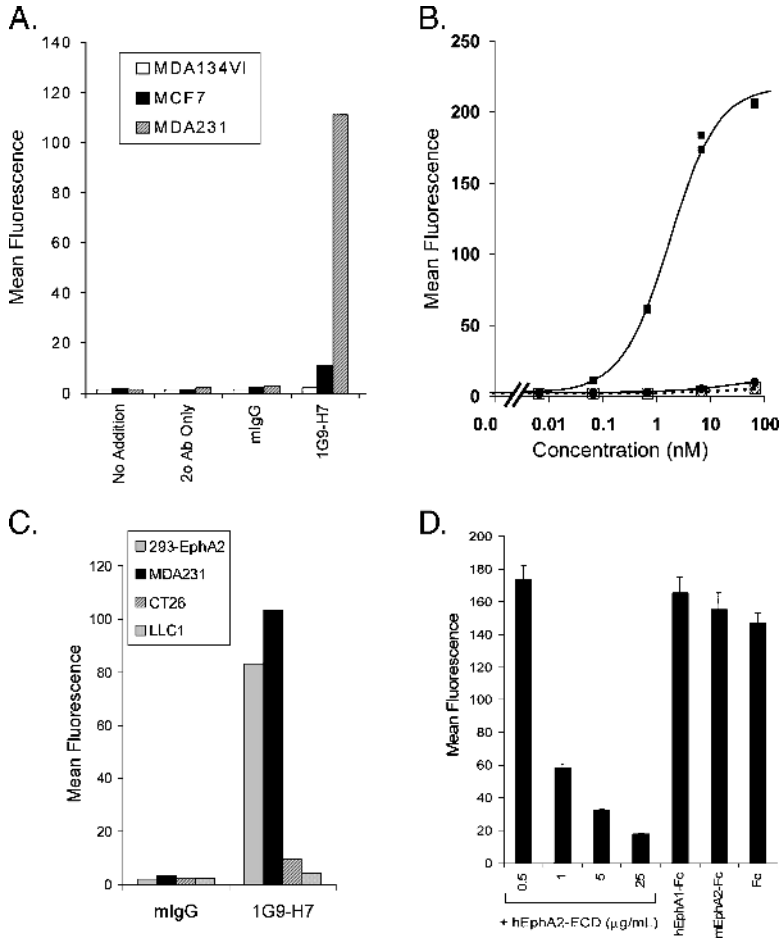

Figure 6. *FACS binding of 1G9-H7 to human EphA2-expressing cells. (A) The indicated human breast cancer cells were incubated in the presence and absence (no addition, secondary Ab only) of 1G9-H7 or normal mouse IgG (2 μg/ml) for 1 hour at 4°C. Primary antibody was detected with anti-mouse IgG Alexa546, and samples were analyzed on a Guava PCA96. The mean fluorescence for each incubation condition is graphically represented. (B) 293 cells (open symbols) and 293-EphA2 cells (solid symbols) were incubated with indicated concentrations of 1G9-H7 (squares) or mIgG (circles), and bound primary antibodies were detected with mouse IgG-Alexa546 by FACS analysis. Mean fluorescence data points for duplicate samples are graphically represented. Calculated EC_{50} = 1.8 nM. (C) Indicated cells were incubated with 2 μg/ml mIgG or 1G9-H7, and bound primary antibodies were detected with anti-mouse IgG Alexa488 by FACS analysis. (D) MDA-231 cells were incubated with 1G9-H7 (2 μg/ml) and indicated concentrations of hEphA2-ECD or the various soluble EphA receptor proteins at 25 μg/ml at 4°C for 1 hour. Cell-bound 1G9-H7 was detected with anti-mouse IgG Alexa546 by FACS analysis. Error bars, SD. The murine IgG secondary antibody does not bind to human Fc (data not shown). Data shown are representative of at least two independent experiments.*

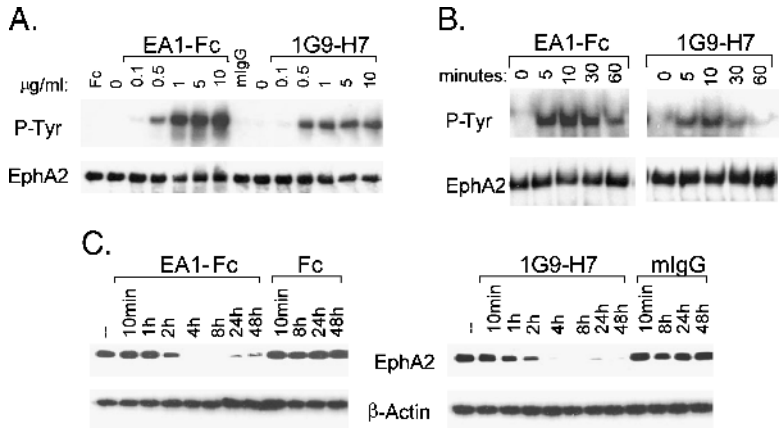

Figure 7. *Comparison of EphA2 activation by 1G9-H7 and EA1-Fc. (A) MDA-231 cells were incubated with 1G9-H7 or EA1-Fc at indicated concentrations for 10 minutes at 37°C. EphA2 in total cell lysates was immunoprecipitated and analyzed by Western blot analysis using either anti-phosphotyrosine (P-Tyr) or anti-EphA2 (C-20) antibodies. Fc and mIgG were incubated at 10 μg/ml. (B) Western blot analysis of immunoprecipitated extracts prepared at the indicated time points following stimulation of MDA-231 cells with 1 μg/ml EA1-Fc or 1G9-H7. (C) The effect of treatment for the indicated times with Fc, EA1-Fc, mIgG, or 1G9-H7 (5 μg/ml) on EphA2 protein levels was evaluated by Western blot analysis using anti-EphA2 (C-20) antibody. Equivalent loading was verified by reprobing the blots with an anti–β-actin antibody. Similar results were observed at 0.5 μg/ml 1G9-H7. Data shown are representative of at least two independent experiments.*

Ab20 showed remarkable similarity to EA1-Fc in its ability to stimulate EphA2 phosphorylation in CT26 colorectal carcinoma cells. As expected for a potent agonist, Ab20 also induced the degradation of EphA2, with time dependency and efficiency similar to those of EA1-Fc. Surprisingly, intraperitoneal administration of Ab20 to mice bearing subcutaneously implanted CT26 tumors had no effect on tumor growth. Yet, the level of EphA2 protein in tumors excised from every one of the Ab20-treated mice was reduced by ~85% relative to levels in tumors from the isotype-treated controls. Moreover, a separate study demonstrated that even a 24-hour treatment with Ab20 was sufficient to substantially reduce tumor EphA2 levels, suggesting that Ab20 accumulated in the tumor and displayed expected EphA2 degradation–

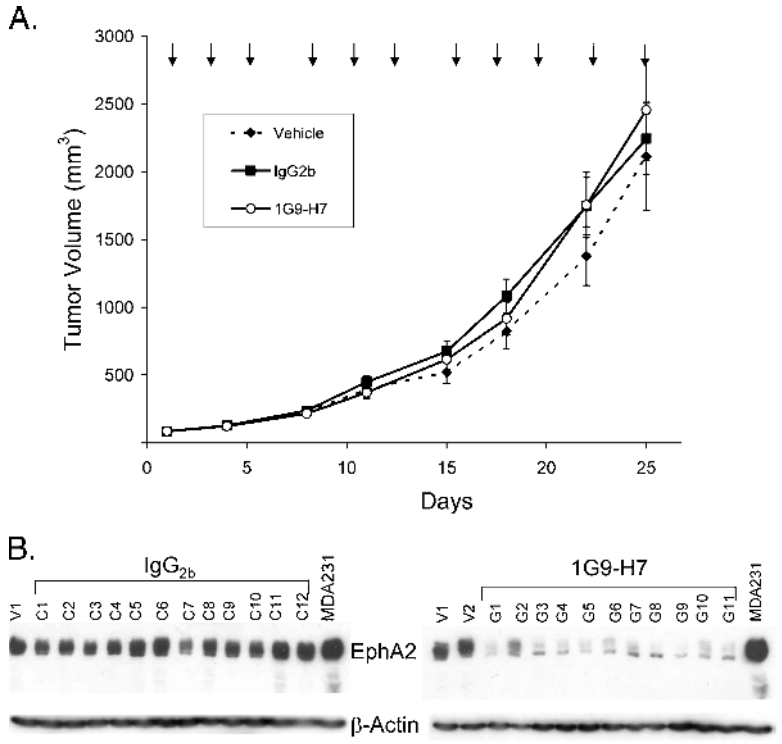

Figure 8. *Effect of anti-human EphA2 antibody 1G9-H7 on MDA-231 tumor growth. (A) Mice bearing MDA-231 orthotopically implanted tumors (50–200 mm^3; n = 12/group) were treated with vehicle, $mIgG_{2b}$, or 1G9-H7 (125 μg/dose) according to the schedule shown (arrows). Mean tumor weights (g) were as follows: vehicle, 1.94 ± 0.36; IgG_{2b}, 2.45 ± 0.28; and 1G9-H7, 2.72 ± 0.52. Error bars, SEM. (B) Western blot analyses of extracts (30 μg of total protein) from the MDA-231 tumors excised from vehicle (V1 and V2)–, $mIgG_{2b}$ (C1–C12)–, or 1G9-H7 (G1–G11)–treated mice probed with anti-EphA2 (C-20) and anti–β-actin antibodies. Average (± SD) EphA2 levels determined by densitometric scanning of the blots: control, 1535 ± 296; and 1G9-H7, 268 ± 89.*

promoting activity shortly after administration. Yet, despite this evidence for the agonistic effects of Ab20 treatment in the tumors, there was no tumor growth inhibition.

The observed *in vitro* inhibitory activity of Ab20 in CT26 tumor cell invasion led us to evaluate its effects on the CT26 cell colonization of the lung. In this study, Ab20 was administered 3 hours prior to the intravenous injection of CT26 cells to enable the binding and activation of EphA2 before the extravasation of tumor cells. Again, Ab20 had no antitumor efficacy, as there was no difference between the tumor burdens in the lungs of Ab20- and IgG_3-treated mice. However, the EphA2 protein levels in the tumor-bearing lungs excised from Ab20-treated mice were barely detectable, whereas high levels were found in the tumors from the isotype control–treated mice. Therefore, despite this evidence for Ab20-elicited EphA2 degradation in lung tumors, no effect on tumor growth was observed. Taken together, these results indicate that high levels of EphA2 are not required for primary CT26 colorectal tumor growth or for tumor cell colonization of the lung. Thus, CT26 colorectal tumors may not be as sensitive to EphA2-targeting agents as the human lung (i.e., A549), breast (i.e., MDA-MB-231), or pancreatic (i.e., MIAPaca-2) tumor xenografts that were inhibited following treatment with agonistic anti-EphA2 antibodies [16] or anti-EphA2 siRNA [18], respectively. It is possible that the residual low levels of EphA2 in the treated CT26 tumor-bearing mice were sufficient for sustaining tumor cell growth *in vivo*, although the reduction of EphA2 observed in our studies is greater than that reported in other studies with different tumor models (see below).

As this study is the first to employ a syngeneic murine tumor model for the evaluation of EphA2 agonists, it is also theoretically possible that inhibitory effects of Ab20 on CT26 tumor cells were opposed by a tumor-promoting activity mediated through host EphA2-expressing cells (e.g., endothelial cells). In this case, the agonistic Ab20 antibody may have stimulated angiogenesis, as it is known that EA1-Fc has stimulatory effects on endothelial cell migration *in vitro* [33] and that ephrinA1 promotes angiogenesis in *in vivo* rat corneal assays [34]. Further studies are needed to clarify relative contributions to the tumor growth of ephrinA–EphA2 signaling activities from host and tumor cells.

An alternative explanation for the lack of efficacy of Ab20 is that oncogenic signaling pathways that are active in CT26 tumor cells are either more critical for *in vivo* tumor growth than those involving EphA2, or enable tumor cells to escape the inhibitory effects of an EphA2 agonist. In this regard, it is of interest that ephrinA1 has been shown to inhibit growth factor–induced—but not constitutively active—Ras/MAP kinase activity in tumor cells [15,35]. If attenuation of MAP kinase activity is important for the growth-inhibitory effects of agonistic antibodies, the presence of activated Ras could make cells resistant to that treatment. Given the frequent occurrence of mutant activated Ras in human colorectal cancers [36], it will be of interest to determine the status of this pathway in CT26 cells.

Prior to initiating studies to evaluate the efficacy of Ab20 in other tumor types, we identified another EphA2 agonistic mAb (1G9-H7) that is similar to EA1-Fc and Ab20 in the potency and kinetics of EphA2 phosphorylation and degradation. However, unlike either of these agonists, 1G9-H7 specifically interacts with hEphA2 as demonstrated by its binding (uniquely) to human cells that express EphA2 and its competition with human—but not murine—EphA2 ECD. 1G9-H7 was tested for its ability to inhibit the growth of orthotopically implanted MDA-231 breast tumors. The selection of this tumor model was influenced by the results published by Coffman et al. [16], who showed that EphA2 agonistic antibodies inhibited MDA-MB-231 and A549 tumor growth by 50% to 60% and also indicated that orthotopically implanted tumors were more responsive than subcutaneously growing tumors. In contrast to their observations, treatment of MDA-231 tumors with the 1G9-H7 antibody failed to affect tumor growth rate. Yet, all of the tumors excised from the 1G9-H7–treated mice had substantially lower levels of EphA2 protein than the isotype-treated controls. These data demonstrate that the 1G9-H7 antibody reached the tumor and induced the degradation of EphA2, thereby suggesting that high levels of EphA2 are not essential for MDA-231 tumor growth. The reduction in EphA2 levels was equal to or greater than that reported by investigators who used anti-EphA2 siRNA or antibodies to decrease EphA2 levels in tumors [13,18]. In the MIAPaca-2 tumor study, the administration of anti-EphA2 siRNA caused an approximately 70% inhibition of tumor growth, and the reduction of EphA2 protein was approximately two-fold relative to controls in the single sample shown [18]. In the MDA-MB-231 tumor study, anti-EphA2 EA2 antibody inhibited tumor growth by ~50%, and the levels of EphA2 in four of eight tumors were undetectable although significant but unquantified levels were found in the remaining tumors [16].

It is possible that the MDA-231 cells that were used in our study were not as dependent on EphA2 for their *in vivo* growth as the cells used in the study by Coffman et al. [16], further emphasizing the importance of determining the molecular characteristics of tumors that make them responsive to anti-EphA2 therapies. Indeed, ephrinA1 treatment stimulated the Ras–MAPK signaling pathway in the MDA-MB-231 cells studied by Pratt and Kinch [37] but had no effect on the MDA-MB-231 cells employed by Mao et al. [35].

It is also conceivable that reduction of EphA2 protein levels may not be the primary determinant of the growth-inhibitory efficacy of EphA2-targeting therapies. Differences in antibodies with respect to EphA2-binding affinity, agonistic potency, site of interaction on the EphA2 protein, and downstream signal transduction may be more important for determining the antitumor efficacy of anti-EphA2 antibodies than previously understood. The EC_{50} for the binding of 1G9-H7 to cell surface hEphA2 is ~2 nM, which is comparable to the reported binding affinity of the EA2 antibody (i.e., 5 nM) [16]. The kinetics of EphA2 degradation in MDA-MB-231 cells induced by the EA2 antibody is also similar to that observed with 1G9-H7. However, the EphA2-activating potency of the EA2 antibody cannot be compared to that of 1G9-H7 because there were no direct comparisons made to EA1-Fc in the published study. As the EphA2 phosphorylation studies

with EA2 were performed at concentrations that were six-fold greater than those required to achieve a maximal phosphorylation of EphA2 with 1G9-H7, it is possible that 1G9-H7 was a more effective agonist than EA2. In this regard, it is noteworthy that the EA2 antibody can bind to EphA2 by ELISA measurement in the presence of EA1-Fc [16]. Thus, EA2 binds to a site on EphA2 that is different from that of the ligand and still functions as an agonist. Our preliminary data indicate that the 1G9-H7 antibody binds to an epitope that overlaps with that of EA1-Fc. It is therefore possible that 1G9-H7 and EA2 may stimulate overlapping yet distinct signal transduction pathways, in conjunction with EphA2 degradation, thereby leading to different abilities to inhibit tumor growth. Thus, induction of EphA2 degradation may not be the only relevant outcome leading to the tumor growth-inhibitory ability of anti-EphA2 antibodies. Future studies to elucidate the signaling pathways evoked by these antibodies will be important for determining the characteristics of EphA2-targeting antibodies that have antitumor properties.

Finally, the specificity of the EA2 antibody toward hEphA2 is unknown. Cross-reactivity with other human or murine ephrin receptors could also enhance the tumor growth–inhibitory activity of this antibody.

In summary, we have generated and characterized two potent agonistic mAbs directed against murine and human EphA2. Following *in vivo* administration of these antibodies, the levels of EphA2 protein in murine CT26 colorectal and human MDA-231 breast tumors were reduced by at least ~80% to 85%, yet no effects on the growth of tumors in the subcutaneous (CT26) or orthotopic (MDA-231) sites, or on tumor cell colonization in the lung (CT26) were observed. Our results indicate that the characteristics of agonistic anti-EphA2 antibodies, in addition to EphA2-degrading ability, may be critical determinants of antitumor activity. This study also suggests that the molecular characterization of tumors for markers that predict responsiveness to anti-EphA2 targeting therapies is warranted.

Acknowledgements

We thank Rene Meisner, Mithra Mahmoudi, and Miriam Schroeder for the pathological evaluation of tumors from efficacy studies, and Kirk McLean for the sequence evaluation of Fab phage display clones. We acknowledge support from Steven Chesney, Kathy White, Jeff Davis, Tim Kenrick, Keith Place, Charles Nguyen, and Alaire DeSalvo for *in vivo* tumor efficacy studies. We appreciate the assistance of Susan Harvey with FACS analysis, and Eileen Paulo-Chrisco, Rhonda Humm, Jean MacRobbie, John Garbutt, and Mary Rosser for cell culture. We also thank Harald Dinter, Gordon Parry, Richard Feldman, and Michael Mamounas for valuable scientific discussions.

References

[1] Kullander K and Klein R (2002). Mechanisms and functions of Eph and ephrin signalling. *Nat Rev Mol Cell Biol* **3,** 475–486.

[2] Surawska H, Ma PC, and Salgia R (2004). The role of ephrins and Eph receptors in cancer. *Cytokine Growth Factor Rev* **15,** 419–433.

[3] Zelinski DP, Zantek ND, Stewart JC, Irizarry AR, and Kinch MS (2001). EphA2 overexpression causes tumorigenesis of mammary epithelial cells. *Cancer Res* **61,** 2301–2306.

[4] Walker-Daniels J, Coffman K, Azimi M, Rhim JS, Bostwick DG, Snyder P, Kerns BJ, Waters DJ, and Kinch MS (1999). Overexpression of the EphA2 tyrosine kinase in prostate cancer. *Prostate* **41,** 275–280.

[5] Thaker PH, Deavers M, Celestino J, Thornton A, Fletcher MS, Landen CN, Kinch MS, Kiener PA, and Sood AK (2004). EphA2 expression is associated with aggressive features in ovarian carcinoma. *Clin Cancer Res* **10,** 5145–5150.

[6] Kinch MS, Moore MB, Harpole DH Jr (2003). Predictive value of the EphA2 receptor tyrosine kinase in lung cancer recurrence and survival. *Clin Cancer Res* **9,** 613–618.

[7] Nakamura R, Kataoka H, Sato N, Kanamori M, Ihara M, Igarashi H, Ravshanov S, Wang YJ, Li ZY, Shimamura T, et al. (2005). EPHA2/EFNA1 expression in human gastric cancer. *Cancer Sci* **96,** 42–47.

[8] Wu D, Suo Z, Kristensen GB, Li S, Troen G, Holm R, and Nesland JM (2004). Prognostic value of EphA2 and EphrinA-1 in squamous cell cervical carcinoma. *Gynecol Oncol* **94,** 312–319.

[9] Nemoto T, Ohashi K, Akashi T, Johnson JD, and Hirokawa K (1997). Overexpression of protein tyrosine kinases in human esophageal cancer. *Pathobiology* **65,** 195–203.

[10] Straume O and Akslen LA (2002). Importance of vascular phenotype by basic fibroblast growth factor, and influence of the angiogenic factors basic fibroblast growth factor/fibroblast growth factor receptor-1 and ephrin-A1/EphA2 on melanoma progression. *Am J Pathol* **160,** 1009–1019.

[11] Saito T, Masuda N, Miyazaki T, Kanoh K, Suzuki H, Shimura T, Asao T, and Kuwano H (2004). Expression of EphA2 and E-cadherin in colorectal cancer: correlation with cancer metastasis. *Oncol Rep* **11,** 605–611.

[12] Zantek ND, Azimi M, Fedor-Chaiken M, Wang B, Brackenbury R, and Kinch MS (1999). E-cadherin regulates the function of the EphA2 receptor tyrosine kinase. *Cell Growth Differ* **10,** 629–638.

[13] Carles-Kinch K, Kilpatrick KE, Stewart JC, and Kinch MS (2002). Antibody targeting of the EphA2 tyrosine kinase inhibits malignant cell behavior. *Cancer Res* **62,** 2840–2847.

[14] Miao H, Burnett E, Kinch M, Simon E, and Wang B (2000). Activation of EphA2 kinase suppresses integrin function and causes focal-adhesion-kinase dephosphorylation. *Nat Cell Biol* **2,** 62–69.

[15] Miao H, Wei BR, Peehl DM, Li Q, Alexandrou T, Schelling JR, Rhim JS, Sedor JR, Burnett E, and Wang B (2001). Activation of EphA receptor tyrosine kinase inhibits the Ras/MAPK pathway. *Nat Cell Biol* **3,** 527–530.

[16] Coffman KT, Hu M, Carles-Kinch K, Tice D, Donacki N, Munyon K, Kifle G, Woods R, Langermann S, Kiener PA, et al. (2003). Differential EphA2 epitope display on normal *versus* malignant cells. *Cancer Res* **63,** 7907–7912.

[17] Hess AR, Seftor EA, Gardner LM, Carles-Kinch K, Schneider GB, Seftor RE, Kinch MS, and Hendrix MJ (2001). Molecular regulation of tumor cell vasculogenic mimicry by tyrosine phosphorylation: role of epithelial cell kinase (Eck/EphA2). *Cancer Res* **61,** 3250–3255.

[18] Duxbury MS, Ito H, Zinner MJ, Ashley SW, and Whang EE (2004). EphA2: a determinant of malignant cellular behavior and a potential therapeutic target in pancreatic adenocarcinoma. *Oncogene* **23,** 1448–1456.

[19] Cheng N, Brantley DM, and Chen J (2002). The ephrins and Eph receptors in angiogenesis. *Cytokine Growth Factor Rev* **13,** 75–85.

[20] Munthe E, Finne EF, and Aasheim HC (2004). Expression and functional effects of Eph receptor tyrosine kinase A family members on Langerhans like dendritic cells. *BMC Immunol* **5,** 9.

[21] de Saint-Vis B, Bouchet C, Gautier G, Valladeau J, Caux C, and Garrone P (2003). Human dendritic cells express neuronal Eph receptor tyrosine kinases: role of EphA2 in regulating adhesion to fibronectin. *Blood* **102,** 4431–4440.

[22] Holzman LB, Marks RM, and Dixit VM (1990). A novel immediate-early response gene of endothelium is induced by cytokines and encodes a secreted protein. *Mol Cell Biol* **10,** 5830–5838.

[23] Sanderson S and Shastri N (1994). LacZ inducible, antigen/MHC-specific T cell hybrids. *Int Immunol* **6,** 369–376.

[24] Zajchowski DA, Bartholdi MF, Gong Y, Webster L, Liu HL, Munishkin A, Beauheim C, Harvey S, Ethier SP, and Johnson PH (2001). Identification of gene expression profiles that predict the aggressive behavior of breast cancer cells. *Cancer Res* **61,** 5168–5178.

[25] Knappik A, Ge L, Honegger A, Pack P, Fischer M, Wellnhofer G, Hoess A, Wolle J, Pluckthun A, and Virnekas B (2000). Fully synthetic human combinatorial antibody libraries (HuCAL) based on modular consen-

sus frameworks and CDRs randomized with trinucleotides. *J Mol Biol* **296,** 57–86.

[26] Krebs B, Rauchenberger R, Reiffert S, Rothe C, Tesar M, Thomassen E, Cao M, Dreier T, Fischer D, Hoss A, et al. (2001). High-throughput generation and engineering of recombinant human antibodies. *J Immunol Methods* **254,** 67–84.

[27] Rauchenberger R, Borges E, Thomassen-Wolf E, Rom E, Adar R, Yaniv Y, Malka M, Chumakov I, Kotzer S, Resnitzky D, et al. (2003). Human combinatorial Fab library yielding specific and functional antibodies against the human fibroblast growth factor receptor 3. *J Biol Chem* **278,** 38194–38205.

[28] Rheinnecker M, Hardt C, Ilag LL, Kufer P, Gruber R, Hoess A, Lupas A, Rottenberger C, Pluckthun A, and Pack P (1996). Multivalent antibody fragments with high functional affinity for a tumor-associated carbohydrate antigen. *J Immunol* **157,** 2989–2997.

[29] Chu YW, Yang PC, Yang SC, Shyu YC, Hendrix MJ, Wu R, and Wu CW (1997). Selection of invasive and metastatic subpopulations from a human lung adenocarcinoma cell line. *Am J Respir Cell Mol Biol* **17,** 353–360.

[30] Roffler SR, Chan J, and Yeh MY (1994). Potentiation of radioimmunotherapy by inhibition of topoisomerase I. *Cancer Res* **54,** 1276–1285.

[31] Chang YW, Chen SC, Cheng EC, Ko YP, Lin YC, Kao YR, Tsay YG, Yang PC, Wu CW, and Roffler SR (2005). CD13 (aminopeptidase N) can associate with tumor-associated antigen L6 and enhance the motility of human lung cancer cells. *Int J Cancer* **5,** 5.

[32] Lindberg RA and Hunter T (1990). cDNA cloning and characterization of eck, an epithelial cell receptor protein-tyrosine kinase in the eph/elk family of protein kinases. *Mol Cell Biol* **10,** 6316–6324.

[33] Cheng N, Brantley DM, Liu H, Lin Q, Enriquez M, Gale N, Yancopoulos G, Cerretti DP, Daniel TO, and Chen J (2002). Blockade of EphA receptor tyrosine kinase activation inhibits vascular endothelial cell growth factor–induced angiogenesis. *Mol Cancer Res* **1,** 2–11.

[34] Pandey A, Shao H, Marks RM, Polverini PJ, and Dixit VM (1995). Role of B61, the ligand for the Eck receptor tyrosine kinase, in TNF-alpha–induced angiogenesis. *Science* **268,** 567–569.

[35] Mao W, Luis E, Ross S, Silva J, Tan C, Crowley C, Chui C, Franz G, Senter P, Koeppen H, et al. (2004). EphB2 as a therapeutic antibody drug target for the treatment of colorectal cancer. *Cancer Res* **64,** 781–788.

[36] Martiny-Baron G, Korff T, Schaffner F, Esser N, Eggstein S, Marme D, and Augustin HG (2004). Inhibition of tumor growth and angiogenesis by soluble EphB4. *Neoplasia* **6,** 248–257.

[37] Pratt RL and Kinch MS (2002). Activation of the EphA2 tyrosine kinase stimulates the MAP/ERK kinase signaling cascade. *Oncogene* **21,** 7690–7699.